DOI: 10.1002/chem.200700126

Heat-Induced Alterations in the Surface Population of Metal Sites in Bimetallic Nanoparticles

Bing-Joe Hwang,*[a, b] Loka Subramanyam Sarma,[a] Guo-Rung Wang,[a] Ching-Hsiang Chen,[a, c] Din-Goa Liu,[b] Hwo-Shuenn Sheu,[b] and Jyh-Fu Lee[b]

Abstract: The ability to alter the surface population of metal sites in bimetallic nanoparticles (NPs) is of great interest in the context of heterogeneous catalysis. Here, we report findings of surface alterations of Pt and Ru metallic sites in bimetallic carbon-supported (PtRu/C) NPs that were induced by employing a controlled thermal-treatment strategy. The thermal-treatment procedure was designed in such a way that the particle size of the initial NPs was not altered and only the surface population of Pt and Ru was changed, thus allowing us to deduce structural information independent of particle-size effects. X-ray absorption spectroscopy (XAS) was utilized to deduce the structural parameters that can provide information on atomic distribution and/or extent of alloying as well as the surface population of Pt and Ru in PtRu/C NPs. The PtRu/C catalyst sample was obtained from Johnson Matthey, and first the as-received catalyst was reduced in 2% H_2 and 98% Ar gas mixture at 300°C for 4 h (PtRu/C as-reduced). Later this sample was subjected to thermal treatment in either oxygen (PtRu/C-O_2-300) or hydrogen (PtRu/C-H_2-350). The XAS results reveal that when the as-reduced PtRu/C catalyst was exposed to the O_2 thermal-treatment strategy, a considerable amount of Ru was moved to the catalyst surface. In contrast, the H_2 thermal-treatment strategy led to a higher population of Pt on the PtRu/C surface. Characterization of the heat-treated PtRu/C samples by X-ray diffraction and transmission electron microscopy reveals that there is no significant change in the particle size of thermally treated samples when compared to the as-received PtRu/C sample. The electrochemical properties of the as-reduced and heat-treated PtRu/C catalyst samples were confirmed by cyclic voltammetry, CO-adsorption stripping voltammetry, and linear sweep voltammetry. Both XAS and electrochemical investigations concluded that the PtRu/C-H_2-350 sample exhibits significant enhancement in reactivity toward methanol oxidation as a result of the increased surface population of the Pt when compared to the PtRu/C-O_2-300 and PtRu/C as-reduced samples.

Keywords: heterogeneous catalysis · platinum · ruthenium · surface chemistry · X-ray absorption spectroscopy

Introduction

The study of the surface composition of bimetallic nanoparticles (NPs) is of fundamental and practical interest in the context of heterogeneous catalysis, as interaction of surface atoms of the catalyst with reactants will play a significant role in catalysis.[1,2] In most cases the surface composition of bimetallic NPs differs from that of the bulk and has a significant influence on NP activity, selectivity, and stability. With the availability of modern techniques, such as low-energy ion-scattering spectroscopy (LEISS), X-ray photoelectron spectroscopy (XPS), and Auger electron spectroscopy (AES), it is possible to obtain reasonably good estimates of the surface composition of solid samples.[3] Among these techniques, LEISS has an outstanding sensitivity toward the outermost atomic layer, whereas XPS and AES can probe the composition of NPs up to a few monolayers. Due to the finite escape depth of the Auger electrons and photoelectrons, the application of AES and XPS to particles with diameters of about or less than 30 Å is restricted.[4,5]

[a] Prof. B.-J. Hwang, Dr. L. S. Sarma, G.-R. Wang, Dr. C.-H. Chen
Department of Chemical Engineering
National Taiwan University of Science and Technology
43 Keelung Road, Section 4, Tapei 106 (Taiwan)
Fax: (+886) 227-376-644
E-mail: bjh@mail.ntust.edu.tw

[b] Prof. B.-J. Hwang, D.-G. Liu, Dr. H.-S. Sheu, Dr. J.-F. Lee
National Synchrotron Radiation Research Center
Hsinchu 30076 (Taiwan)

[c] Dr. C.-H. Chen
Institute of Atomic and Molecular Sciences
Academia Sinica, Taipei 106 (Taiwan)

Among the different bimetallic systems, the carbon-supported Pt–Ru system (PtRu/C) has received renewed interest from both the scientific and industrial communities, due to its suitability as a catalyst for methanol oxidation in direct methanol fuel cells (DMFCs).[6–9] The optimum catalytic activity is strongly dependent on the atomic-scale distribution of Pt and Ru sites in the catalyst matrix,[10–13] as well as the surface composition and particle size of the alloy particles.[14] Studies that involve the alteration of surface composition are very impressive in the context of DMFC research. However, it is difficult to study the effect of surface composition on catalytic reactions independently without interference resulting from the variation of particle size. Numerous heat-treatment strategies have been reported in the literature with the aim to improve the catalytic activity of PtRu/C NPs toward methanol oxidation[15–18] and CO tolerance.[19–21] Babu et al.[15] observed that thermal treatment on PtRu/C NPs in a hydrogen atmosphere at 220 °C can enhance the CO tolerance and methanol oxidation reactivity as a result of the maximum number of Pt–Ru contacts on the alloy overlayer. On the other hand, Raman and coworkers[16] found that annealing PtRu/C NPs between 250 and 300 °C in air for 30 min is beneficial in improving the methanol oxidation activity. They attributed this finding to a positive variation in Ru/Pt ratio due to the diffusion of Ru metal from the bulk catalyst to the surface with an increase in oxidic ruthenium content. These results are quite controversial, as they did not consider the variation in particle size that arises from the heat treatment in realizing the effect of surface population on catalytic activity. It prompted us to look at another way of studying the effect of the surface composition of PtRu/C catalyst without changing its particle size. In a theoretical work of Han et al.[22] on adsorbate-controlled surface segregation, it was proposed that adsorbed oxygen on Pt–Ru induces surface segregation of Ru due to the strong binding between Ru and O on the surface. Moreover, it was demonstrated that the Ru component has a higher heat of adsorption of O_2, whereas the Pt component has a higher heat of adsorption of H_2.[23]

Motivated by these studies, here we developed a controlled thermal-treatment strategy to alter the surface population of Pt and Ru without varying the particle size of the initial PtRu/C NPs. The controlled heating and cooling cycles employed in this study allowed us to induce changes in the surface Pt and Ru population. Estimation of the surface population of Pt and Ru NPs is rather difficult with the available surface-sensitive techniques, such as scanning tunneling microscopy (STM), LEISS, or AES, as these techniques are suitable for the estimation of the Pt and Ru composition of bulk alloy surfaces.[24–27] X-ray diffraction (XRD) can provide information on the atomic composition of Pt and Ru in the bulk but not at the surface of the NP.[28,29] Early reports have highlighted the use of infrared spectroscopy for the determination of the surface composition of Pt–Ru bimetallic NPs.[30,31] Dinh et al. have determined the surface composition of both supported and unsupported Pt–Ru catalyst NPs by employing CO stripping voltammetry as a surface diagnostic tool.[32] Their method relies on the data of Gasteiger et al. on the CO stripping voltammetry of well-characterized bulk Pt–Ru alloy electrode surfaces.[33] Recently, Yeh et al. explored the surface composition of PtRu/C alloy crystallites by temperature-programmed reduction (TPR).[34] X-ray absorption fine structure (XAFS) spectroscopy has proven to be an appropriate technique for estimating alloy formation and surface composition in the bimetallic NPs and offers possibilities to understand the heterogeneous catalysis process on nanoscale Pt–M, where M is a 4d transition metal.[35,36] In the case of nanoscale materials, due to the small particle size (1–3 nm) the number of surface atoms is large (for example, if the particle size is 2.5 nm the number of surface atoms per total number of atoms in the particle is 50 %).[37] Due to the very large fraction of the total number of atoms that reside either at or near the surface, the application of X-ray absorption spectroscopy (XAS) to such a nanoscale system can provide information on surface properties.[38] By comparing the average number of Pt–Pt ($N_{\text{Pt-Pt}}$) and Pt–Ru ($N_{\text{Pt-Ru}}$) atom pairs obtained from Pt L_{III}-edge XAS data with the average coordination number of Ru–Ru ($N_{\text{Ru-Ru}}$) and Ru–Pt ($N_{\text{Ru-Pt}}$) obtained from Ru K-edge XAS, it is possible to obtain qualitative information on the Pt and Ru surface population and quantitative information on the extent of alloying and/or atomic distribution of Pt (J_{Pt}) and Ru (J_{Ru}) in PtRu/C NPs.

Thus, the overall objective of the present study is to alter the surface population of Pt and Ru in the PtRu/C catalyst matrix without varying the particle size, by using a controlled thermal-treatment strategy. The corresponding changes that occurred in the extent of alloying and/or J_{Pt} and J_{Ru} in PtRu/C NPs, which are induced by heat treatment in O_2 and H_2 environments, are analyzed from the XAS results. The observed changes in J_{Pt} and J_{Ru} are then correlated to the electrochemical performance of PtRu/C NPs. From the XAS and electrochemical results of this study, we observed that even slight changes in J_{Pt}, J_{Ru}, and the surface Pt and Ru population that are induced by heat treatment have a significant influence on the catalyst activity toward the methanol oxidation reaction.

Results and Discussion

The XRD patterns for as-reduced PtRu/C and the PtRu/C catalyst samples heat-treated in O_2 and H_2 atmospheres are shown in Figure 1. All the XRD patterns clearly show face-centered-cubic (fcc) crystalline Pt (JCPDS card 4-802), namely, the planes (111), (200), (220), (311), and (222). However, these signals are slightly shifted to a higher angle, which is consistent with alloying to Ru metal. The average size of the heat-treated PtRu/C catalyst samples was estimated by using the Scherrer equation[39] $d = 0.94\lambda_{k\alpha 1}/B_{(2\theta)}\cos\theta_B$, where d is the average particle diameter, $\lambda_{k\alpha 1}$ is the wavelength of X-ray radiation (0.15406 nm), θ_B is the angle of the (220) peak, and $B_{(2\theta)}$ is the width in radians of the diffraction peak at half-height. The obtained average

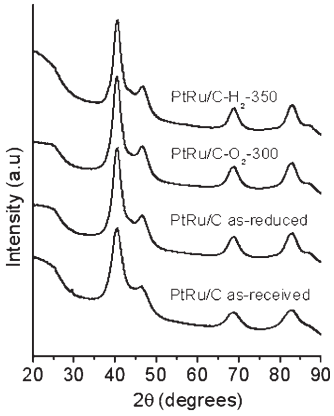

Figure 1. XRD patterns for PtRu/C NPs as-received, as-reduced, heat-treated in O_2, and heat-treated in H_2 atmospheres. Energy for excitation: 25 keV; wavelength (λ): 0.5167 Å.

particle sizes of all the catalysts are given in Table 1. It can be seen that there is no significant change in the grain size of all the heat-treated PtRu/C catalyst samples in the present study. Due to the presence of amorphous Ru oxide in the case of as-received PtRu/C, the calculated grain size is smaller. These results indicate that the controlled thermal-treatment strategy employed in this study does not influence the particle size of the initial PtRu/C catalyst NPs.

Table 1. Comparison of grain size and particle diameter obtained through XRD and TEM data, respectively, of PtRu/C NPs as-received, as-reduced, and heat-treated in O_2 and H_2 atmospheres.

Sample conditions	Grain size from XRD [nm]	Particle diameter from TEM [nm]
as-received PtRu/C	2.8	3–4
as-reduced PtRu/C	3.1	3–4
PtRu/C-O_2-300	3.1	3–4
PtRu/C-H_2-350	3.1	3–4

Figure 2 displays transmission electron microscopy (TEM) images of PtRu/C catalysts under various conditions. In all the conditions studied, particles with an average diameter of approximately 3–4 nm are uniformly distributed on the carbon support, thus providing further evidence that the controlled thermal-treatment strategy employed in the present study does not alter the particle size of the initial PtRu/C NPs (Table 1). These results are in agreement with the XRD measurements.

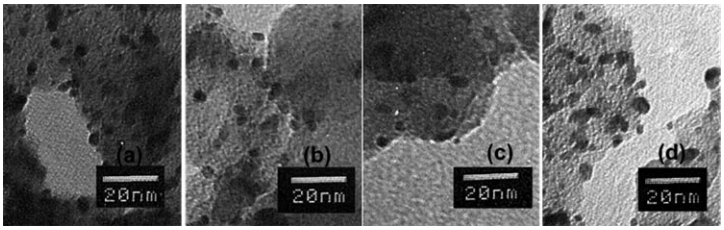

Figure 2. TEM images of a) as-received and b) as-reduced PtRu/C NPs; c) PtRu/C-O_2-300 and d) PtRu/C-H_2-350 samples.

Evaluation of Pt and Ru atomic distribution changes by XAS: XAS measurements comprising both the X-ray absorption near-edge structure (XANES) and extended X-ray absorption fine structure (EXAFS) regions were performed on PtRu/C catalyst samples. XANES can provide information about the electronic state of the atoms in the material, while EXAFS provides valuable structural and chemical information on the neighborhood of the excited atom, particularly coordination numbers and bond distances. XANES spectra of PtRu/C catalyst samples under various conditions of treatment recorded at the Pt L_{III}-edge and Ru K-edge are shown in Figure 3a and b, respectively. The white-line intensity for the PtRu/C catalyst in O_2 treatment conditions is higher than that of the Pt reference foil. However, the intensity of the white line of the as-reduced PtRu/C catalyst and PtRu/C-H_2-350 samples is lower when compared to that of

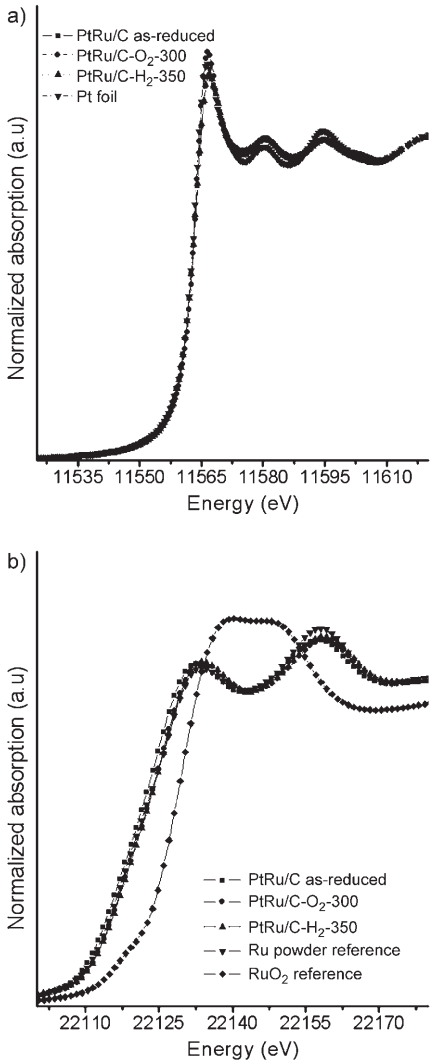

Figure 3. XANES spectra of as-reduced and heat-treated PtRu/C catalysts recorded at the a) Pt L_{III}-edge and b) Ru K-edge.

the Pt reference foil. The white line is attributed to the excitation of the $2p_{3/2}$ core electron to the unoccupied 5d states near the Fermi level, and its magnitude is directly related to the occupancy of the 5d electronic states.[40–42] In order to obtain reasonable structural parameters from XAS for PtRu/C samples, particles should be in the metallic state.[10] The XANES results presented here show that the as-reduced and thermally treated catalysts are in the metallic state.

The Ru K-edge XANES spectra of as-reduced and heat-treated PtRu/C samples, along with those of relevant reference compounds, are shown in Figure 3b. The XANES spectrum of ruthenium oxide (Ru^{4+}) shows a 6-eV positive edge shift when compared to the Ru metal powder reference. The edge shifts of the as-reduced and heat-treated catalyst samples approach more toward the Ru metal reference, which indicates a zero-valent character of the Ru component in the catalyst and rules out the possibility of a Ru oxidic nature in the samples.

The imaginary part and real magnitude of the Fourier transform (FT) of experimental EXAFS data at the Pt L_{III}-edge for PtRu/C as-reduced, PtRu/C-O_2-300, and PtRu/C-H_2-350 samples are shown in Figure 4a, c, and e along with the *R*-space fit. Similarly, the imaginary part and real magnitude of the FT of experimental EXAFS data at the Ru K-edge for PtRu/C as-reduced, PtRu/C-O_2-300, and PtRu/C-H_2-350 samples are shown in Figure 4b, d and f along with the *R*-space fit. However, for clarity in the FT intensity changes, the FT data of the EXAFS spectra at the Pt L_{III}-edge and Ru K-edge of the PtRu/C catalyst samples under various conditions are compared in Figure 5a and b.

Structural parameters, for example, interatomic distance (R), coordination number (N), and Debye–Waller factor ($\Delta\sigma_i^2$), for the PtRu/C catalyst are obtained from the EXAFS refinement and are summarized in Tables 2 and 3. The EXAFS data for the two edges were fitted simultaneously. For all the PtRu/C catalyst samples, the coordination numbers of unlike atom pairs ($N_{\text{Pt-Ru}}$ and $N_{\text{Ru-Pt}}$) were further constrained to match each other. In the FT-EXAFS spectra at the Pt L_{III}-edge (Figure 5a), a strong peak appeared between 2 and 3 Å with a splitting that results from the Pt–Pt and Pt–Ru interactions, and the appearance of this peak is consistent with the reported spectra for other related Pt–Ru catalysts.[43–45] The intensity of the peak resulting from the Pt–Pt and Pt–Ru interactions is almost same in the case of PtRu/C as-reduced and PtRu/C-H_2-350 samples, whereas it is increased in the case of the PtRu/C-O_2-300 sample. The increased FT intensity implies a higher contribution of Pt coordination in the core region. These results suggest that a considerable number of Ru atoms in the PtRu/C-O_2-300 sample have moved to the surface, thereby giving a predominant population of Pt in the core region. The Ru preference for the surface upon O_2 treatment of PtRu/C is consistent with the theoretical predictions of Han et al.[22] The FT-EXAFS spectra at the Ru K-edge (Figure 5b) also exhibit a peak in the *R* range of 2–3 Å due to the first-shell metal–metal bonding involving Ru–Pt and Ru–Ru correlations. In this case, the intensity of the peak related to the Ru–Ru first coordination shell splitting is higher for the PtRu/C-H_2-350 sample. This finding indicates that Pt atoms present in the core are brought to the surface of the clusters upon H_2 treatment, and as a result a higher population of Ru atoms is present in the core region.

Recently, we have shown that the structure of bimetallic catalysts can be significantly influenced by the degree of alloying between the two constituent elements and influences their catalytic activity. An XAS-based methodology has been developed to determine the atomic distribution or extent of alloying of bimetallic NPs and to show their impact on catalytic activity.[10] We have applied this methodology to PtRu/C catalyst samples treated under various conditions. First, we calculated the total number of Pt and Ru atoms around Pt ($\Sigma N_{\text{Pt-}i} = N_{\text{Pt–Pt}} + N_{\text{Pt–Ru}}$) and the total number of Ru and Pt atoms around Ru ($\Sigma N_{\text{Ru-}i} = N_{\text{Ru–Ru}} + N_{\text{Ru–Pt}}$). From these values the structural parameters that can provide quantitative information about the atomic distribution in bimetallic clusters, such as P_{observed} ($N_{\text{Pt–Ru}}/\Sigma N_{\text{Pt-}i}$) and R_{observed} ($N_{\text{Ru-Pt}}/\Sigma N_{\text{Ru-}i}$), can be determined. By using the P_{observed} and R_{observed} values, the extent of alloying of Pt (J_{Pt}) and Ru (J_{Ru}) can then be calculated from Equations (1) and (2), respectively.

$$J_{\text{Pt}} = (P_{\text{observed}}/P_{\text{random}}) \times 100 \quad (1)$$

$$J_{\text{Ru}} = (R_{\text{observed}}/R_{\text{random}}) \times 100 \quad (2)$$

where P_{random} and R_{random} can be taken as 0.5 for perfectly alloyed bimetallic NPs if the atomic ratio of "Pt" and "Ru" is 1:1. This value can be achieved by assuming that $N_{\text{Pt–Pt}} = N_{\text{Pt–Ru}}$ and $N_{\text{Ru–Ru}} = N_{\text{Ru–Pt}}$, which is generally true for perfectly alloyed bimetallic NPs. The ratio of $\Sigma N_{\text{Pt-}i}$ to $\Sigma N_{\text{Ru-}i}$ ($Q = \sum_i N_{\text{Pt}-i} / \sum_i N_{\text{Ru-}i}$) is also an important parameter to assess the structure of the bimetallic NPs. If the Q value is higher than 1 then the catalyst possesses a Pt-rich$_{\text{core}}$–Ru-rich$_{\text{shell}}$ structure, and if the value is lower than 1 the reverse is true. If the Q value shows any positive or negative deviation from unity, it can provide information on the relative population of the core and shell components. We have listed the $\Sigma N_{\text{Pt-}i}$, $\Sigma N_{Ru\text{-}i}$, P_{observed}, R_{observed}, J_{Pt}, J_{Ru}, and Q values for all the PtRu/C catalysts treated under various conditions in Table 4.

A common observation found for as-reduced and heat-treated PtRu/C catalysts is that $\Sigma N_{\text{Pt-}i} > \Sigma N_{\text{Ru-}i}$, $J_{\text{Ru}} > J_{\text{Pt}}$, and $Q > 1$ (see Table 4). The standard errors presented for all the parameters are significantly low. It has been shown in the literature that if a homogeneous system of A–B bimetallic NPs follows the relationship of $N_{\text{A–A}} + N_{\text{A–B}} > N_{\text{B–A}} + N_{\text{B–B}}$, then the core of the cluster is composed of N atoms of A (N_{A}) and the surface is made of N atoms of B (N_{B}); the total coordination number ($N_{\text{A–A}} + N_{\text{A–B}}$) for the "A" atom is greater than that for the "B" atom ($N_{\text{B–A}} + N_{\text{B–B}}$), and this hypothesis is based on the absence of monometallic clusters.[46–48] Hence, the observed parameter relationship, that

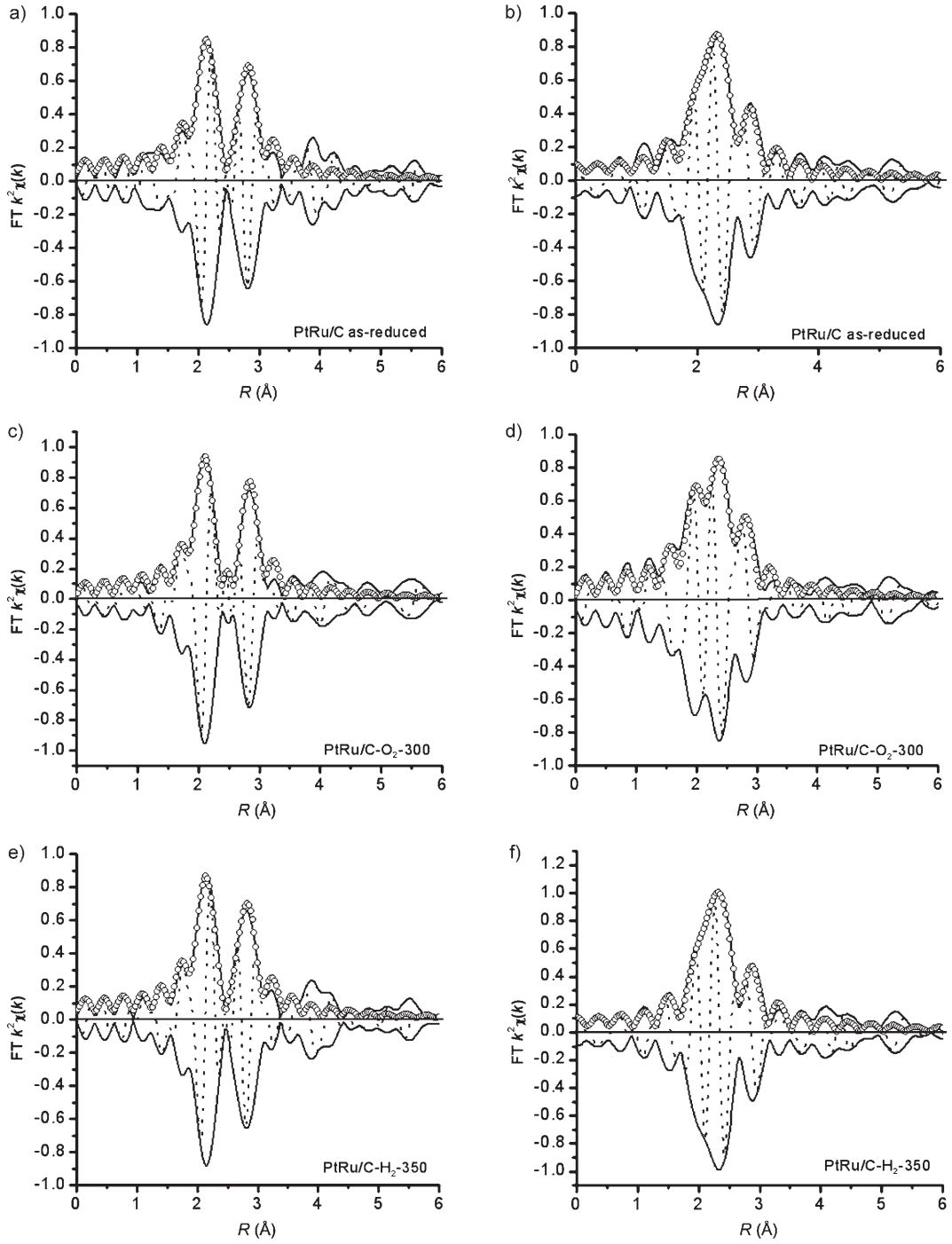

Figure 4. Imaginary part (——) and real magnitude of FT (k^2-weighted) of experimental EXAFS data (-----) and fits (○). a,c,e) Data at the Pt L_{III}-edge for PtRu/C as-reduced, PtRu/C-O_2-300, and PtRu/C-H_2-350, respectively. b,d,f) Data at the Ru K-edge for PtRu/C as-reduced, PtRu-O_2-300, and PtRu/C-H_2-350, respectively.

is, $\Sigma N_{\text{Pt-i}} > \Sigma N_{\text{Ru-}i}$ supports the Pt-rich$_{\text{core}}$–Ru-rich$_{\text{shell}}$ structure for all the PtRu/C NPs investigated here. Even though the structures of the as-reduced and heat-treated PtRu/C catalysts appear to be similar, the structural parameters P_{observed}, R_{observed}, J_{Pt}, and J_{Ru} show small but significant changes from the as-reduced to heat-treated conditions, which needs a detailed explanation.

In the case of as-reduced PtRu/C, the J_{Pt} and J_{Ru} values are found to be 61 and 75%, respectively. The lower J_{Pt} value reveals that in the core, homometallic Pt–Pt bonds are preferred rather than heterometallic Pt–Ru bonds. The larger J_{Ru} value indicates that most of the Ru is involved in alloying, and hence there is less segregation of Ru in the shell region. The lower P_{observed} value of 0.30 when compared

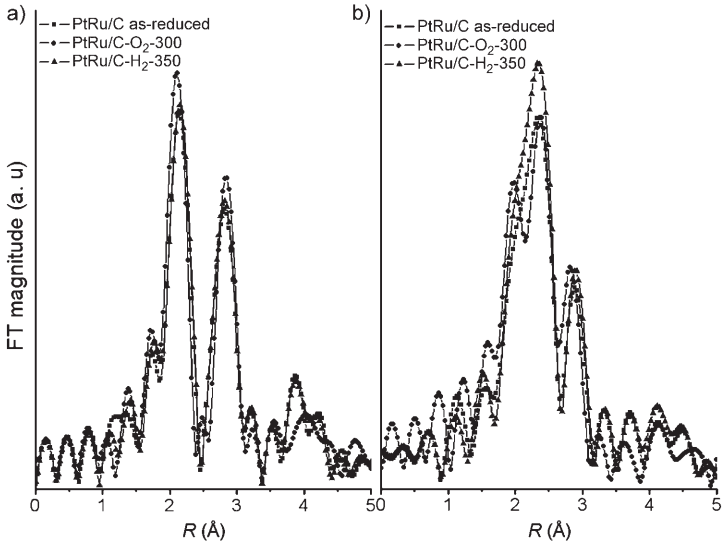

Figure 5. FT of k^2-weighted EXAFS data for as-reduced and heat-treated PtRu/C catalyst samples: a) at Pt L_{III}-edge and b) at Ru K-edge.

Table 2. EXAFS fitting parameters at the Pt L_{III}-edge for PtRu/C catalysts under various conditions.[a]

Sample	Shell	N	R [Å]	$\Delta\sigma_j^2$ [Å^2]	ΔE_0 [eV]	R factor
as-reduced PtRu/C	Pt–Ru	2.7	2.719	0.005	6.6	
		(±0.1)	(±0.006)	(±0.0008)	(±1.2)	
	Pt–Pt	6.2	2.739	0.006	5.7	0.005
		(±0.2)	(±0.006)	(±0.0004)	(±1.1)	
PtRu/C-O_2-300	Pt–Ru	2.7	2.711	0.005	4.5	
		(±0.4)	(±0.006)	(±0.0009)	(±1.3)	
	Pt–Pt	6.0	2.741	0.006	5.3	0.006
		(±0.5)	(±0.007)	(±0.0006)	(±1.2)	
PtRu/C-H_2-350	Pt–Ru	2.7	2.722	0.004	7.2	
		(±0.1)	(±0.004)	(±0.0007)	(±0.9)	
	Pt–Pt	6.1	2.739	0.005	5.8	
		(±0.2)	(±0.005)	(±0.0003)	(±0.9)	0.005

[a] Notation: N, coordination number; R, distance between absorber and backscatterer atoms; $\Delta\sigma_j^2$, Debye–Waller factor; ΔE_0, inner potential corrections. The error bounds stated here were obtained from the statistical analysis of the data by FEFFIT software.

Table 3. EXAFS fitting parameters at the Ru K-edge for PtRu/C catalysts under various conditions.[a]

Sample	Shell	N	R [Å]	$\Delta\sigma_j^2$ [Å^2]	ΔE_0 [eV]	R factor
as-reduced PtRu/C	Ru–Ru	4.5	2.678	0.005	2.3	
		(±0.2)	(±0.006)	(±0.0008)	(±1.1)	
	Ru–Pt	2.7	2.719	0.004	2.0	0.005
		(±0.1)	(±0.006)	(±0.0001)	(±1.1)	
PtRu/C-O_2-300	Ru–Ru	4.0	2.675	0.005	1.4	
		(±0.4)	(±0.005)	(±0.0006)	(±0.8)	
	Ru–Pt	2.7	2.711	0.004	1.0	0.006
		(±0.4)	(±0.006)	(±0.0010)	(±1.7)	
PtRu/C-H_2-350	Ru–Ru	4.7	2.677	0.005	1.3	
		(±0.2)	(±0.005)	(±0.0003)	(±0.9)	
	Ru–Pt	2.7	2.722	0.003	2.0	0.005
		(±0.1)	(±0.006)	(±0.0008)	(±1.1)	

[a] Notation as in Table 2.

Table 4. Extent of alloying and atomic distribution parameters of bimetallic PtRu/C catalysts treated under various conditions.

Sample	$\Sigma N_{Pt\text{-}i}$	$\Sigma N_{Ru\text{-}i}$	P_{obs}	R_{obs}	J_{Pt} [%]	J_{Ru} [%]	Q
as-reduced PtRu/C	8.9	7.2	0.30	0.38	61	75	1.24
PtRu/C-O_2-300	8.7	6.7	0.31	0.40	62	80	1.30
PtRu/C-H_2-350	8.8	7.4	0.31	0.36	61	73	1.20

to the $R_{observed}$ value of 0.38 for the as-reduced PtRu/C catalyst suggests that a considerable amount of Pt is segregated in the core region, whereas a lesser amount of Ru is segregated in the shell region. When the catalyst is subjected to heat treatment in an O_2 atmosphere, significant changes are observed in both the segregation and extent of alloying parameters. An increase in J_{Pt} and J_{Ru} values is observed, but the increase in J_{Ru} is more pronounced. The total coordination number of Pt and Ru around Ru, that is, $\Sigma N_{Ru\text{-}i}$, is decreased to 6.7 in the case of the PtRu/C-O_2-300 sample from the 7.2 of as-reduced PtRu/C. The decrease in $\Sigma N_{Ru\text{-}i}$ indicates that the Ru on the surface increases. Hence, it is reasonable to expect that the surface composition of Ru is increased in the case of the PtRu/C-O_2-300 sample. The changes in atomic distribution and extent of alloying are different in the case of the sample treated in a H_2 atmosphere. In this case no change in the extent of alloying of Pt and a significant decrease in the extent of alloying of Ru are observed when compared to the PtRu/C catalyst in the as-reduced state, thus indicating that Ru may be moved to the core region whereas the Pt is moved to the shell region, and thereby an increase in the surface composition of Pt can be expected.

Cyclic voltammetry (CV) can provide some information about the state of the surface of metal NPs. Figure 6 compares the voltammograms of PtRu/C NPs as-reduced and heat-treated in O_2 and H_2 atmospheres. Currents are expressed in terms of geometric surface area. In the hydrogen region (from 0 to 0.33 V vs. NHE) corresponding to the reductive adsorption of protons in the cathodic scan and the subsequent oxidation of the hydrogen adatoms in the anodic scan, the CV peak seems to be slightly more defined for the catalyst submitted to thermal treatment in a H_2 atmosphere (PtRu/C-H_2-350). This kind of CV feature can generally be observed for a sample in which the population of Pt sites is more pronounced on the surface.[21] It indicates that the PtRu/C-H_2-

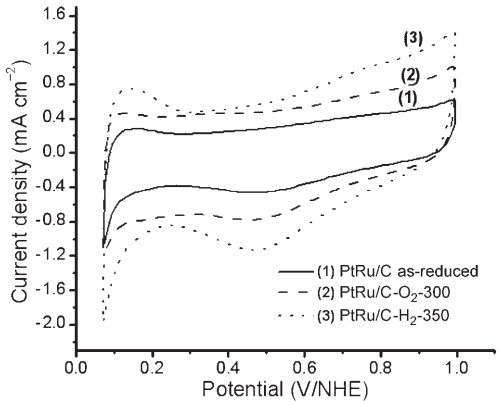

Figure 6. Cyclic voltammograms of PtRu/C catalysts under various conditions recorded in 0.5 M H_2SO_4 with a scan rate of 10 mV s^{-1} at 40 °C. NHE: normal hydrogen electrode.

350 catalyst NPs may contain a considerable amount of Pt on their surfaces and is consistent with the XAS results presented herein. The lack of a H_2 adsorption/desorption peak is more significant in PtRu/C-O_2-300 when compared to the PtRu/C as-reduced sample. The cyclic voltammograms of PtRu/C as-reduced and PtRu/C-O_2-300 samples are close to the features of Ru-rich Pt–Ru samples.[49] However, the increased current in the case of the Ru-rich PtRu/C-O_2-300 sample may arise due to the surface roughening caused by the oxidative treatment. We did not attempt to calculate the electrochemically active surface area of the catalysts from the H_2 desorption region, as the onset of Ru oxide formation before the "double-layer" region at about 350 mV hinders the exact determination of the H_2 desorption region. However, as can be seen from the cyclic voltammograms, from the increase of charges in both the hydrogen and oxide regions we expect a higher electrochemical surface area for the PtRu/C-H_2-350 sample.

Figure 7 shows the CO stripping voltammograms for all three samples. The CO stripping peak of as-reduced PtRu/C and PtRu/C-H_2-350 samples is positioned at 0.41 V. However, for the sample treated in an O_2 atmosphere, that is, PtRu/C-O_2-300, the CO stripping peak is shifted positively by 30 mV. A prewave observed on the PtRu/C-H_2-350 sample was attributed to the oxidation of weakly adsorbed CO.[20,50] The appearance of a prepeak in the case of the H_2-treated catalyst suggests that the catalyst may have facile sites for CO oxidation at low potentials. The CO oxidation onset potential (E_{on}), anodic peak for CO_{ads} oxidation to CO_2 (E_{pa}), and peak current density for all three catalyst samples are listed in Table 5. As can be seen, the onset potential of PtRu/C-H_2-350 is significantly lower when compared to those of the as-reduced and PtRu/C-O_2-300 samples, and it has a high CO oxidation peak current density. The increased catalytic activity of PtRu/C-H_2-350 is due to the increased population of Pt on the surface, as revealed by the XAS results.

Figure 8 shows cyclic voltammograms for methanol oxidation over PtRu/C as-reduced, PtRu/C-O_2-300, and PtRu/C-

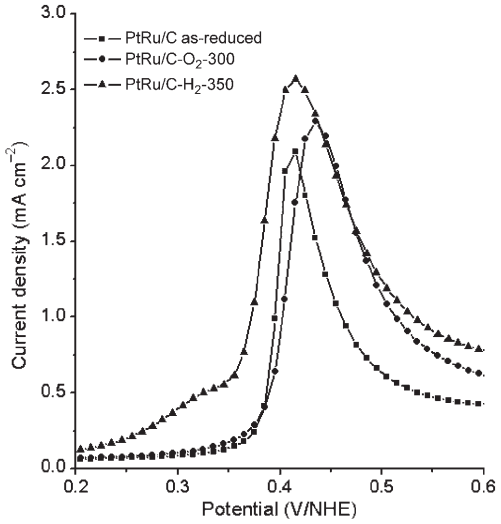

Figure 7. Stripping curves for CO oxidation on as-reduced and heat-treated PtRu/C catalyst samples with adsorption of CO at 0.05 V versus NHE followed by N_2 bubbling for 15 min. Scan rate: 5 mV s^{-1}; electrolyte: 0.5 M H_2SO_4; temperature: 40 °C.

Table 5. Comparative performance of PtRu/C catalyst samples treated under various conditions.[a]

Sample	E_{on} [V]	E_{pa} [V]	Peak current density [mA cm^{-2}]
PtRu/C as-reduced	0.37	0.41	1.94
PtRu/C-O_2-300	0.38	0.44	2.06
PtRu/C-H_2-350	0.33	0.41	2.31

[a] E_{on}, onset potential for the CO_{ads} to CO_2 oxidation; E_{pa}, anodic peak for the CO_{ads} to CO_2 oxidation.

H_2-350 samples in a solution of 0.5 M H_2SO_4 and 10 vol% CH_3OH at 40 °C. The onset potential for methanol oxidation for PtRu/C-H_2-350 occurred at a lower anodic potential (0.34 V vs. NHE) than that for the PtRu/C-O_2-300 (0.40 V vs. NHE) and PtRu/C as-reduced samples (0.38 V vs. NHE). The peak current densities associated with methanol oxidation in the forward scan for PtRu/C as-reduced, PtRu/C-O_2-

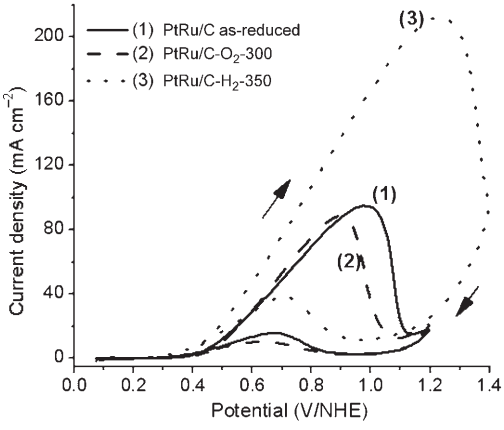

Figure 8. Cyclic voltammograms of PtRu/C catalysts under various conditions recorded in 0.5 M H_2SO_4 + 10 vol% CH_3OH solution with a scan rate of 10 mV s^{-1} at 40 °C.

300, and PtRu/C-H_2-350 were found to be 88, 95, and 213.9 mA cm^{-2}, respectively. At a potential interesting for DMFC applications, that is, at 0.45 V versus NHE, the current densities for PtRu/C as-reduced, PtRu/C-O_2-300, and PtRu/C-H_2-350 were found to be 6.2, 4.3, and 12.6 mA cm^{-2}, respectively. These results suggest that the methanol oxidation activity of PtRu/C-H_2-350 is significantly higher than that of PtRu/C as-reduced and PtRu/C-O_2-300 samples. As can be seen from the XAS results, a considerable fraction of Pt atoms in the core of the PtRu/C-H_2-50 sample have moved to the shell region and thereby increased the surface Pt–Ru contacts. The increased catalytic activity of this sample is, therefore, most likely due to the increase in the number of surface Pt atoms. In contrast, the XAS results of PtRu/C-O_2-300 reveal that Ru atoms migrate to the surface and are responsible for the decreased methanol oxidation activity.

Figure 9 shows the linear sweep voltammograms for methanol electrooxidation on the PtRu/C catalysts. The PtRu/C catalyst submitted to H_2 thermal treatment, that is, PtRu/C-H_2-350, exhibits a higher mass-specific activity (41.15 mA per mg Pt) at 0.45 V versus NHE. The PtRu/C-O_2-300 and PtRu/C as-reduced samples exhibited lower mass-specific activities of 13.98 and 13.08, respectively, at 0.45 V versus NHE. The comparative tests concluded that PtRu/C-H_2-350 had the best electrocatalytic performance in relation to the other two PtRu/C catalysts.

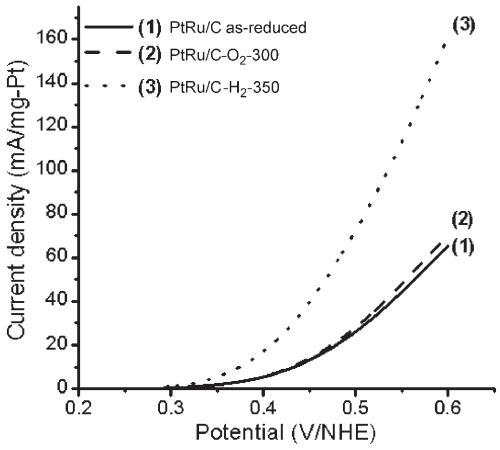

Figure 9. Linear sweep voltammograms of PtRu/C as-reduced, PtRu/C-O_2-300, and PtRu/C-H_2-350 samples recorded in 0.5 M H_2SO_4 + 10 vol% CH_3OH solution at 40 °C. Scan rate: 0.07 mV s^{-1}; rotation rate: 2500 rpm.

Conclusion

We have shown that the XAS results obtained in this study can provide qualitative information on the surface composition of Pt and Ru in bimetallic PtRu/C NPs. The thermal-treatment strategy can control the surface population of Pt and Ru in PtRu/C catalyst NPs without changing the size of the initial particles. The XAS results reveal that heat treatment in an O_2 atmosphere (PtRu/C-O_2-300) can draw the Ru present in the core of the cluster to the surface. In contrast, heat treatment in a H_2 atmosphere (PtRu/C-H_2-350) led to the migration of core Pt to the shell region. The corresponding electrochemical investigations clearly demonstrate that the PtRu/C-H_2-350 sample exhibits higher methanol oxidation activity as a result of an increased surface population of Pt when compared to PtRu/C as-reduced and PtRu/C-O_2-300 samples. Although the present thermal-treatment strategy induces Pt and Ru surface population changes in a narrow range, further enhancement of the surface population of Pt and Ru in a wider range in PtRu/C catalysts for higher methanol oxidation activity can be expected by performing repeated thermal-cycling experiments on PtRu/C NPs. The results reported here are of general interest, as they apply not only to PtRu/C NPs but also to other kinds of bimetallic NPs.

Experimental Section

Thermal treatment of PtRu/C NPs: A commercial Johnson Matthey HiSPEC 5000 PtRu/C (20 wt% Pt and 10 wt% Ru) catalyst was used for the thermal treatment studies. To obtain a reliable comparison, samples from the same batch with homogeneous mixing were used. First, the as-received catalyst powder was reduced at 300 °C for about 4 h under a flow of gaseous mixture containing 2% H_2 and 98% Ar. The Ar was purged for 2 h and the sample was allowed to cool to room temperature and was labeled PtRu/C as-reduced. In the case of O_2 thermal treatment experiments, pure O_2 gas was introduced into the sample chamber with a flow rate of 60 mL min^{-1} for about 30 min to allow O_2 adsorption onto the sample. Later, Ar gas was purged for 20 min to remove any excess of O_2 present in the system and then the temperature was raised to 300 °C and held for 1 h. Again, Ar was purged for 30 min and then the sample was cooled to room temperature. This sample was referred to as PtRu/C-O_2-300. In a similar way H_2 thermal-cycling experiments were performed on the as-reduced catalyst by purging with pure H_2 at room temperature and raising the temperature to 350 °C. The sample was held at 350 °C for 1 h and Ar gas was purged for about 30 min prior to cooling to room temperature. The sample obtained at this stage was denoted as PtRu/C-H_2-350.

XRD: High-energy XRD measurements on the catalyst samples were made at the beam line BL01C2 at the National Synchrotron Radiation Research Center (NSRRC), Hsinchu, Taiwan. The beam line was operated with an energy of 25 keV. The XRD pattern was recorded using a wavelength (λ) of 0.5167 Å for limited angular regions at room temperature. The wavelength was changed to 1.5418 Å as the energy of $Cu_{K\alpha}$. The spectra were obtained at a scan rate of 10° min^{-1}, with steps of 0.05° in the 2θ scans from 20 to 90°.

TEM: TEM was performed on a JEOL JEM 1010 microscope operating at 80 kV. Samples were prepared by sonicating a small amount of the catalyst NPs in ethanol. A drop of this slurry was deposited onto a holey carbon–copper grid, and the ethanol was allowed to evaporate. The samples were examined at 200 k magnification.

XAS measurements: The X-ray absorption spectra were recorded at the Taiwan beam line BL12B2, at the Spring-8, Hyogo, Japan, and at BL01C at the NSRRC, Hsinchu, Taiwan. The electron storage ring of Spring-8 was operated at 8 GeV. A double Si(111) crystal monochromator was employed for energy selection with a resolution $\Delta E/E$ better than 1×10^{-4} at both the Pt L_{III}-edge (11564 eV) and the Ru K-edge (22117 eV). All of the spectra were recorded at room temperature in transmission mode. Higher harmonics were eliminated by detuning the double crystal Si(111) monochromator. Three gas-filled ionization chambers were used in series

to measure the intensities of the incident beam (I_0), the beam transmitted by the sample (I_t), and the beam subsequently transmitted by the reference foil (I_r). The third ion chamber was used in conjunction with a reference sample, which was a Pt foil for Pt L_{III}-edge measurements and Ru powder for Ru K-edge measurements. The control of parameters for EXAFS measurements, data collection modes, and calculation of errors were all carried out according to the guidelines set by the International XAFS Society Standards and Criteria Committee.[51,52]

XAS data analysis: We carried out systematic analysis on all the PtRu/C samples studied here by employing similar XAS data treatment procedures. Standard procedures were followed to analyze the XAS data. First, the raw absorption spectrum in the preedge region was fitted to a straight line and the background above the edge was fitted with a cubic spline. The edge position was calibrated by using Pt foil and Ru powder references for Pt and Ru edges, respectively. The EXAFS function χ was obtained by subtracting the postedge background from the overall absorption and then normalized with respect to the edge jump step. The normalized $\chi(E)$ was transformed from energy space to k-space, where "k" is the photoelectron wave vector. The $\chi(k)$ data were multiplied by k^2 to compensate the damping of EXAFS oscillations in the high-k region. Subsequently, k^2-weighted $\chi(k)$ data in the k-space ranging from 3.6 to 12.6 $Å^{-1}$ for the Pt L_{III}-edge and from 3.6 to 11.6 $Å^{-1}$ for the Ru K-edge were Fourier transformed to r-space to separate the EXAFS contributions from the different coordination shells. A nonlinear least-squares algorithm was applied to the curve fitting of an EXAFS spectrum in the r-space between 1.2 and 3.2 Å (without phase correction) for Pt, and between 1.0 and 3.2 Å for Ru. The applied fit ranges allowed the number of independent parameters (N_{ind}) to be 13.5 and 13.2 for the Pt L_{III}-edge and Ru K-edge fits, respectively, according to the Nyquist theorem [Eq. (3)]:[53]

$$N_{ind} = (2\Delta R\Delta k/\pi) + 2 \quad (3)$$

The Pt–Ru reference file was determined by a theoretical calculation. All the computer programs were implemented in the UWXAFS 3.0 package[54] with the backscattering amplitude and the phase shift for the specific atom pairs being theoretically calculated by using FEFF7 code.[55] From these analyses structural parameters, such as coordination number (N), bond distance (R), Debye–Waller factor ($\Delta\sigma_j^2$), and inner potential shift (ΔE_0), have been calculated. Values of the amplitude reduction factor S_0^2 for Pt and Ru were obtained by analyzing the Pt foil and Ru powder reference samples, respectively, and by fixing the coordination number in the FEFFIT input file. The S_0^2 values were found to be 0.905 and 0.880 for Pt and Ru, respectively, after preliminary refinements. The values of residual factor (R-factor) are less than 10, indicating that errors associated with data fitting are quite small [Eq. (4)]:

$$\text{Residual factor } (\%) = \frac{\sum_{i=1}^{N} |\gamma_{exp}(i) - \gamma_{theo}(i)|}{\sum_{i=1}^{N} |\gamma_{exp}(i)|} \times 100 \quad (4)$$

The error bounds in the fit parameters N, R, $\Delta\sigma_j^2$, and ΔE_0 were obtained from the 95% confidence level using FEFFIT software.[56] The standard errors for the coordination numbers at the 95% confidence interval were calculated by dividing the error bounds for each coordination number by a factor of 1.96. These standard errors were used to calculate the standard errors for the addition, ratio, and percentage of coordination numbers by employing the appropriate statistical equations.

Electrochemical measurements: Electrochemical measurements were carried out using a conventional three-electrode electrochemical cell at 40 °C. The working electrode was made of the heat-treated PtRu/C catalyst sample immobilized on a glassy carbon (GC) surface (0.1964 cm^2). The procedure for electrode fabrication involved: 1) preparing a clear suspension of catalyst ink by sonicating a known amount of catalyst powder dispersed in 0.5 wt% Nafion; 2) placing an aliquot of the suspension (7 μL) on a GC disk; and 3) air-drying the disk for about 5 min at room temperature and then at 80 °C to yield a uniform thin film of the catalyst. A high-surface-area Pt electrode and a saturated calomel electrode (SCE) were used as counter and reference electrodes, respectively. However, all potentials reported herein are referenced to the NHE. The CV experiments were performed in 0.5 M H_2SO_4 solution in the presence of 10 vol% CH_3OH at a scan rate of 10 $mV s^{-1}$ with a Solartron 1480 voltammetric analyzer. N_2 gas was purged for nearly 30 min before starting the experiment, and stable voltammograms recorded after ten cycles were taken into account for all the CV experiments. Linear sweep voltammetry was performed in the range from 0.05 to 0.6 V in a solution of 0.5 M H_2SO_4 and 10 vol% CH_3OH with a scan rate of 0.07 $mV s^{-1}$.

CO stripping experiments: A CO voltammetric stripping experiment was performed as follows. CO was adsorbed onto the electrode surface by bubbling high-purity CO through 0.5 M H_2SO_4 for 15 min, while holding the electrode potential at 50 mV versus NHE. After the adsorption period, the dissolved CO was removed from the solution by bubbling high-purity nitrogen for 15 min while still holding the potential at 50 mV. The potential was then cycled at 5 $mV s^{-1}$ starting at 0.07 V versus NHE for two complete cycles.

Acknowledgements

The authors gratefully acknowledge the financial support from the National Science Council, and facilities from the National Synchrotron Radiation Research Center (NSRRC) and the National Taiwan University of Science and Technology, Taiwan.

[1] C. M. Grill, R. D. Gonzalez, *J. Catal.* **1980**, *64*, 487.
[2] B. Zhou, S. Hermans, G. A. Somorjai, *Nanotechnology in Catalysts*, Kluwer Academic/Plenum, New York, **2004**.
[3] P. N. Ross, *Electrochim. Acta* **1991**, *36*, 2053.
[4] C. Powell, *Quantitative Surface Analysis of Materials* (Ed.: N. S. McIntyre), ASTM Special Publication 643, American Society for Testing and Materials, Philadelphia, **1978**, p. 5.
[5] D. Briggs, M. P. Seah, *Practical Surface Analysis, Vol. 1*, Wiley, New York, **1990**.
[6] T. J. Schmidt, H. A. Gasteiger, R. J. Behm, *Electrochem. Commun.* **1999**, *1*, 1.
[7] A. Kabbabi, R. Faure, R. Durand, B. Beden, F. Hahn, J.-M. Léger, C. Lamy, *J. Electroanal. Chem.* **1998**, *444*, 41.
[8] H. N. Dinh, X. Ren, F. H. Garzon, P. Zelenay, S. Gottesfeld, *J. Electroanal. Chem.* **2000**, *491*, 222.
[9] L. S. Sarma, T.-D. Lin, Y.-W. Tsai, J.-M. Chen, B.-J. Hwang, *J. Power Sources* **2005**, *139*, 44.
[10] B.-J. Hwang, L. S. Sarma, J.-M. Chen, C.-H. Chen, S.-C. Shih, G.-R. Wang, D.-G. Liu, J.-F. Lee, M.-T. Tang, *J. Am. Chem. Soc.* **2005**, *127*, 11140.
[11] J.-M. Chen, L. S. Sarma, C.-H. Chen, M.-Y. Cheng, S.-C. Shih, G.-R. Wang, D.-G. Liu, J.-F. Lee, M.-T. Tang, B.-J. Hwang, *J. Power Sources* **2006**, *159*, 29.
[12] C. Bock, C. Paquet, M. Couillard, G. A. Botton, B. R. MacDougall, *J. Am. Chem. Soc.* **2004**, *126*, 8028.
[13] T. Iwasita, H. Hoster, A. John-Anacker, W. F. Lin, W. Vielstich, *Langmuir* **2000**, *16*, 522.
[14] H. A. Gasteiger, N. Markovic, P. N. Ross, E. J. Cairns, *J. Phys. Chem.* **1993**, *97*, 12020.
[15] P. K. Babu, H. S. Kim, S. T. Kuk, J. H. Chung, E. Oldfield, A. Wieckowski, *J. Phys. Chem. B* **2005**, *109*, 17192.
[16] R. K. Raman, A. K. Shukla, A. Gayen, M. S. Hegde, K. R. Priolkar, P. R. Sarode, S. Emura, *J. Power Sources* **2006**, *157*, 45.
[17] H. Qiao, M. Kunimatsu, N. Fujiwara, T. Okada, *Electrochem. Solid-State Lett.* **2005**, *8*, A175.
[18] A. H. C. Sirk, J. M. Hill, K. Y. S. Kung, V. I. Birss, *J. Phys. Chem. B* **2004**, *108*, 689.
[19] A. M. Castro Luna, G. A. Camara, A. Paganin, E. A. Ticianelli, E. R. Gonzalez, *Electrochem. Commun.* **2000**, *2*, 222.

[20] F. Colmati, Jr., W. H. Lizcano-Valbuena, G. A. Camara, E. A. Ticianelli, E. R. Gonzalez, *J. Braz. Chem. Soc.* **2002**, *13*, 474.
[21] G. A. Camara, M. J. Giz, V. A. Paganin, E. A. Ticianelli, *J. Electroanal. Chem.* **2002**, *537*, 21.
[22] B. C. Han, A. van der Ven, G. Ceder, B.-J. Hwang, *Phys. Rev. B* **2005**, *72*, 205409.
[23] B. D. McNicol, R. T. Short, *J. Electroanal. Chem.* **1977**, *81*, 249.
[24] K. Friedrich, K. P. Geyzers, A. J. Dickinson, U. Stimming, *J. Electroanal. Chem.* **2002**, *524–525*, 261.
[25] G. Filho-Tremilios, H. Kim, W. Chrzanowski, A. Wieckowski, B. Grzybowska, P. Kulesza, *J. Electroanal. Chem.* **1999**, *467*, 143.
[26] H. A. Gasteiger, N. Markovic, P. N. Ross, Jr., E. J. Cairns, *J. Electrochem. Soc.* **1994**, *141*, 1795.
[27] E. Herrero, J. M. Feliu, A. Wieckowski, *Langmuir* **1999**, *15*, 4944.
[28] Z. Jusys, T. J. Schmidt, L. Dubau, K. Lasch, L. Jorissen, J. Garche, R. J. Behm, *J. Power Sources* **2002**, *105*, 297.
[29] T. J. Schmidt, H. A. Gasteiger, R. J. Behm, *Electrochem. Commun.* **1999**, *1*, 1.
[30] P. Ramamoorthy, R. D. Gonzalez, *J. Catal.* **1979**, *58*, 188.
[31] H. Miura, T. Suzuki, Y. Ushikubo, K. Sugiyama, T. Matsuda, R. D. Gonzalez, *J. Catal.* **1984**, *85*, 331.
[32] H. N. Dinh, X. Ren, F. H. Garzon, P. Zelenay, S. Gottesfeld, *J. Electroanal. Chem.* **2000**, *491*, 222.
[33] H. A. Gasteiger, N. Markovic, P. N. Ross, Jr., E. J. Cairns, *J. Phys. Chem.* **1994**, *98*, 617.
[34] S.-Y. Huang, S.-M. Chang, C.-T. Yeh, *J. Phys. Chem. B* **2006**, *110*, 234.
[35] P. L. Hansen, M. A. Molenbroek, A. V. Ruban, *J. Phys. Chem. B* **1997**, *101*, 1861.
[36] D. Bazin, C. Mottet, G. Tréglin, *Appl. Catal. A* **2000**, *200*, 47.
[37] R. E. Benfield, *J. Chem. Soc. Faraday Trans.* **1992**, *88*, 1107.
[38] A. I. Frenkel, C. Wills, R. G. Nuzzo, *J. Phys. Chem. B* **2001**, *105*, 12689.
[39] R. J. Matyi, L. H. Schwartz, J. B. Butt, *Catal. Rev. Sci. Eng.* **1987**, *29*, 41.
[40] J. H. Sinfelt, G. D. Meitzner, *Acc. Chem. Res.* **1993**, *26*, 1.
[41] J. McBreen, S. Mukerjee, *J. Electrochem. Soc.* **1995**, *142*, 3399.
[42] M.-K. Min, J. Cho, K. Cho, H. Kim, *Electrochim. Acta* **2000**, *45*, 4211.
[43] A. E. Russell, S. Maniguet, R. J. Mathew, J. Yao, M. A. Roberts, D. Thompsett, *J. Power Sources* **2001**, *96*, 226.
[44] M. S. Nashner, A. I. Frenkel, D. L. Adler, J. R. Shapley, R. G. Nuzzo, *J. Am. Chem. Soc.* **1997**, *119*, 7760.
[45] M. S. Nashner, A. I. Frenkel, D. Somerville, C. W. Hills, J. R. Shapley, R. G. Nuzzo, *J. Am. Chem. Soc.* **1998**, *120*, 8093.
[46] G. H. Via, J. H. Sinfelt in: *X-ray Absorption Fine Structure for Catalysts and Surfaces* (Ed.: Y. Iwasawa), World Scientific, London, **1996**.
[47] D. Bazin, D. Sayers, J. J. Rehr, *J. Phys. Chem. B* **1997**, *101*, 11040.
[48] D. Bazin, D. Guillaume, Ch. Pichon, D. Uzio, S. Lopez, *Oil Gas Sci. Technol.* **2005**, *5*, 801.
[49] B. R. Rauhe, Jr., F. R. McLarnon, E. J. Cairns, *J. Electrochem. Soc.* **1995**, *142*, 1073.
[50] E. Herrero, J. M. Feliu, A. Aldaz, *J. Electroanal. Chem.* **1996**, *368*, 101.
[51] See, for example, the guidelines for data collection modes for EXAFS measurements and user-controlled parameters at http://ixs.iit.edu/subcommittee_reports/sc/sc00report.pdf
[52] Guidelines for error reporting can be found at http://ixs.iit.edu/subcommittee_reports/sc/err-rep.pdf
[53] E. A. Stern, *Phys. Rev. B* **1993**, *48*, 9825.
[54] F. A. Stern, M. Newville, B. Ravel, Y. Yacoby, D. Haskel, *Physica B* **1995**, *208–209*, 117.
[55] S. Zabinsky, J. J. Rehr, A. L. Ankudinov, R. C. Albers, M. Eller, *Phys. Rev. B* **1995**, *52*, 2995.
[56] M. Newville, R. Ravel, D. Haskel, J. J. Rehr, E. E. Stern, Y. Yacoby, *Physica B* **1995**, *208–209*, 154.

Received: January 24, 2007
Published online: April 26, 2007

